International Journal of Bio-Inorganic Hybrid Nanomaterials

pH and Properties of Synthesized Barium Hexa-Ferrite by Co-precipitation Method

Shaghayagh Marzban[1*], Saeid Abedini Khorrami[2]

[1] *M.Sc. Student, Department of Chemistry, Tehran North Branch, Islamic Azad University, Tehran, Iran*

[2] *Associate Professor, Department of Chemistry, Tehran North Branch, Islamic Azad University, Tehran, Iran*

ABSTRACT

Synthesis of $BaFe_{12}O_{19}$ magnetic nano particles via precipitation in different pH conditions have been reported. The certain molar ratio of Fe/Ba = 12 selected and sodium hydroxide was used as a precipitant agent. X-ray Diffraction (XRD), Scanning Electron Microscopy (SEM) and vibrating sample magnetometer (VSM) were used to consider the structural, morphological and magnetic properties of barium hexaferrite nano-particles, respectively. Results demonstrated that pH plays an important role in phase composition; so affected sample properties. The broad hysteresis loop shows that the barium hexaferrite powder was in good crystalline nature.

Keyword: Barium Hexaferrite; Co-precipitaion; pH; Magnetic Properties; Nanoparticles; Hard Ferrites; XRD.

1. INTRODUCTION

Barium ferrites are well known as a hard magnetic material, which are based on iron oxides. They are technologically noteworthy, because of their excellent properties such as chemical stability, corrosion resistivity and high coercive force. Because of these they could not be easily replaced by any other magnets [1, 2]. Hexagonal ferrites are a wide family of ferromagnetic oxides. The crystal structure of the different known types of hexagonal ferrites (M, W, X, Y, Z and U) is very complex and can be considered as a superposition of R and S blocks along the hexagonal c axis, RSR*S* for M-type [3]. They have potential application in contrast agent in magnetic resonance imaging (MRI), recording media, radar absorbing material and as microwave absorber materials [4-6]. Some of the other applications are applied as Flame retardant in plastics, coatings, fiber and textiles [7]. Conventional preparing methods of M type barium ferrite nanoparticles, such as ball milling rout, requires a high calcination temperature around 1200-1300°C and uses a mild mixture of barium carbonate

salt and ferric oxide. Furthermore, these processes result in entrance of impurities into the compositions, generation of lattice strains in the molecular structure and made irregularity in the particle shape. The high temperature insures the formation of barium ferrite; larger particles are also produced in this process [8, 9]. Nowadays, Ba hexa-ferrites are obtained by different chemical methods such as hydrothermal [10, 11], sol-gel auto-combustion [12,13], co-precipitation [14-17]. Among these methods, co-precipitation is one of the simplest techniques. This method uses accessible, environment-friendly and cheap precursors such as chlorides and nitrates salts and sodium hydroxide. This process accrues at lower temperature conditions so, known as green synthesis methods. In the present work, $BaFe_{12}O_{19}$ powder has been prepared by co-precipitation method using metallic nitrates of barium and iron as precursors. Characterization of nano-particles showed the success process.

2. EXPERIMENTAL

2.1. Materials

Barium nitrate $Ba(NO_3)_2$ (99%, Merck), ferric nitrate nona hydrated $Fe(NO_3)_3 \cdot 9H_2O$ (99%, Merck) and sodium hydroxide used as starting materials without any purification. Deionized water applied in preparing all solutions.

2.2. Synthesis of BaFe₁₂O₁₉

Synthesis of nano-sized powder of magnetic barium hexaferrite was carried out as follows: Appropriate amounts of $Fe(NO_3)_3 \cdot 9H_2O$, $Ba(NO_3)_2$ kept at a molar ratio of 12:1. The salt solution was added dropwise to the base solution until the pH reached at 8, 10 and 12 for each system, respectively. The red precipitates were washed and filtered repeatedly with distilled water. This process took about 6 hours. The sample was then dried in an oven, keeping temperature at 80°C for 3 hours. After attaining the powder by mortar and pestle, calculation process was carried out at 1000°C for 2 hours to get the final product.

2.3. Characterization process

X-ray diffraction (XRD) pattern was measured by a

"Philips X'pert", using Cu Kα radiation at 40 kV and 30 mA. A "Philips XL-30" scanning electron microscope was used to characterize the morphologies and microstructure of the samples.

3. RESULTS AND DISCUSSION

The phase identification of the nano-powders was recorded by X-ray diffraction with Cu-Kα radiation source in the range of the 2θ Bragg angle= 20-70°. The X-ray patterns of sample powders C_1, C_2 and C_3 prepared at pH= 8, 10 and 12 are shown in Figure 1. The well matched picks with reference JCPDS NO. 74-1121 picks show that $BaFe_{12}O_{19}$ with miller plates (1 1 4) and (1 0 7), is dominant phase in all of samples. In Figure 1 the miller plates (1 1 0) and (1 0 4) refers to the small amount of α-Fe_2O_3 as sub phase in sample C_1 (synthesized at pH 8). Also the matched pick with (2 1 2) demonstrates that $BaFe_2O_4$ is impurity phase at sample C_2 (synthesized at pH 10). As shown in Figure 1. the absence of any sub-picks demonstrates that C3 (synthesized at pH 12) has a good $BaFe_{12}O_{19}$

Figure 1: *X-ray diffraction pattern of $BaFe_{12}O_{19}$ synthesis in different pH.*

Table 1: *Crystallinity percent, particle size and phases of samples prepare in different pH.*

Sample	Ba:Fe	pH	Phases	Particles size (nm)	Percent Crystallinity (%)
C_1	1:10	8	Fe_2O_3, $BaFe_{12}O_{19}$	35.58	49.45
C_2	1:10	10	Fe_2O_3, $BaFe_2O_4$, $BaFe_{12}O_{19}$	39.25	57.83
C_3	1:10	12	$BaFe_{12}O_{19}$	44.28	58.80

Table 2: *Magnetic parameters of $BaFe_{12}O_{19}$ nanopowders prepared at pH= 12.*

Sample	Ba:Fe	pH	M_s(emu g^{-1})	M_r(emu g^{-1})	H_c(Oe)
C_3	1:10	12	45.8	29.4	3746.9

single phase composition.

The crystallite powders size was also measured by X-ray line broadening technique using the Scherer's formula indicated in Equation (1):

$$d = 0.9\lambda / \beta \cos\theta \qquad \text{(Eq. 1)}$$

Where D is the grain diameter, β is half-intensity width of the relevant diffraction, λ is X-ray wavelength and θ the diffraction angle.

The results revealed that the number of phases, particle size and percent cristallinity of $BaFe_{12}O_{19}$ hexagonal structures are influenced by changing pH. XRD pattern shows that hexagonal structures at selected pH 8, 10, and 12 are the main structure. Number of phases
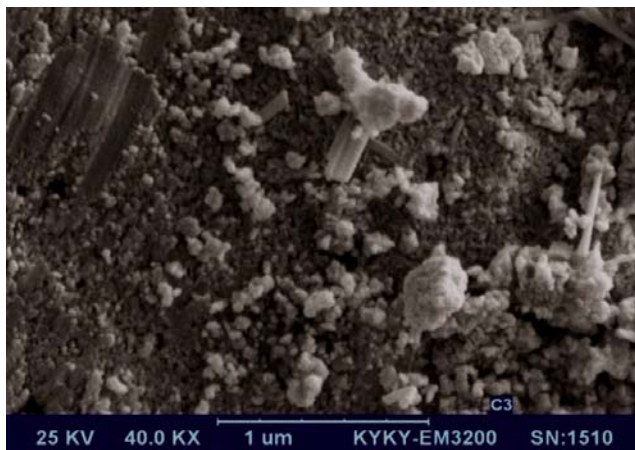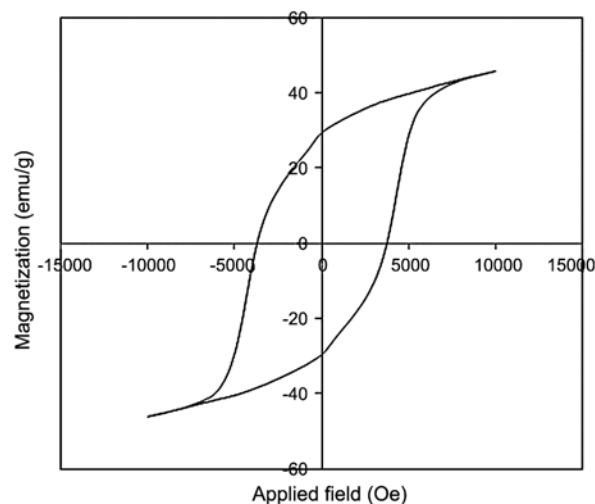
Figure 3: *VSM Loop of $BaFe_{12}O_{19}$ nano-particles synthesized in pH= 12.*

decrease with the pH rising. The effect of pH on the average size and percent crystallinity of nanoparticles is summarized in Table 1.

As shown in Figure 2 the synthesized $BaFe_{12}O_{19}$ nanoparticles at pH= 12 has nonregular shape morphology at all. It was observed that individual grains are not distributed homogenously, but rather tend to agglomerate forming larger bundles. But another interest is starting of formation of hexagonal shapes at high level pH. The magnetic properties were measured by using VSM with an applied field of 3T at room temperature. Plot of magnetization (M) as a function of applied magnetic field (H) is shown in Fig-

Figure 2: *SEM imagining of $BaFe_{12}O_{19}$ nano-particles synthesized in pH= 12.*

ure 3. The smooth hysteresis loop confirm with X-ray results demonstrated the formation of the pure barium hexa-ferrite. The magnetic properties such as saturation magnetization (M_s), remanent magnetization (M_r) and cervicitis (H_c) of sample C_3, reported in Table 2. Even though from the SEM analysis particles are not uniformly distributed but the particle size and particle morphology are the main reasons for the low coercivity ($H_c = 3746.9$).

4. CONCLUSIONS

Single phase barium hexa-ferrite powder was synthesized successfully by co-precipitation technique. Results demonstrate that pH plays an important role in the phase formation process. As by pH value increasing, the main phase composition growing up and at last single phase obtained at pH= 12. Magnetic properties of sample C_3 as a hard magnet, by single phase composition based on XRD data series, indicate and confirm with what we expected from with literatures.

REFERENCES

1. Nowosieslski R., Babilas R., Dercz G., Pajak L., Skowronski W., *JAMME*, **27** (2009), 51.
2. Valenzuela R., *Phys. Res. Inter.*, Article ID: 591839, (2012), 1.
3. Pullar R.C., *Prog. Mater. Sci.,* **57** (2012), 1191.
4. Wang Y., Huang Y., Wang Q., He Q., Chen L., *Appl. Surf. Sci.*, **259** (2012), 486.
5. Ozah S., Bhattacharyya N.S., *J. Magn. Mater.*, **342** (2013), 92.
6. Li Q., Pang J., Wang B., Tao D., Xu X., Sun L., Zhai J., *Adv. Powder Technol.*, **24** (2013), 288.
7. Aksit A.C., Onar N., Ebeoglugil M.F., Birlik I., Celik E., Ozdemir E., *J. appl. Polym. Sci.*, **113** (2009), 358.
8. Stablin H., Wohlfrath E.P. (Eds), Ferromagnetic Materials, North-Holland, *Amsterdam*, **3** (1982), 87.
9. Xu G., Ma H., Zhong M., Zhiu J., You Y., He Zh., *J. Magn. Mater.*, **301** (2006), 383.
10. Drofenik M., Ban I., Makovec D., Znidarsic A., Jaglicic Z., Hanzel D., Lisjak D., *Mater. Chem. Phys.*, **127** (2011), 415.
11. Janasi S.R., Emura M., Landgraf F.J.G., Rodrigues D., *J. Magn. Mater.*, **238** (2002), 168.
12. Adschiri T., Hakuta Y., Arai K., *Ind. Eng. Chem. Res.*, **39** (2000), 4901.
13. Mali A., Ataie A., *J. Al. Com.*, **399** (2005), 245.
14. (a) Packiaraj G., Nital P., Jotania R.B., *J. Biomed. Bioeng.*, **1** (2010), 1. (b) Liu Y., Zhang H., Liu Y., Wang L., Li Y., *Adv. Mater. Res.*, **3052** (2011), 239.
15. Chen D.H., Chen Y.Y., *J. Colloid. Inter f. Sci.*, **235** (2001), 9.
16. Mallick K.K., Shepherd Ph., Green R.J., *J. Eur. Ceram. Soc.*, **27** (2007), 2045.
17. Rashad M.M., Ibrahim I.A., *J. Magn. Mater.*, **323** (2011), 2158.